Experimental investigation of clogging mechanism of pervious concrete made with variable aggregate gradations

◉M. Nazeer, ◉K. Kapoor✉, ◉S.P. Singh

Dr. B.R. Ambedkar National Institute of Technology Jalandhar, (Punjab, India)
✉: kapoork@nitj.ac.in

ABSTRACT: In this study, the clogging mechanism of pervious concrete was evaluated using three different cloggers such as, Sand (S), Clay (C), and combination of sand and clay (S &C). The clogging mechanism was performed through falling head permeability apparatus, using clogger sediment load at the rate of 50, 150, and 200 grams in repetitive clogging cycles. It was observed from the results that combined (S & C) clogger shows overall critical results of clogging as 80% of the clogging was seen in 3 to 4 cycles. Moreover, it was observed from the results that pervious concrete mix made with R- type of aggregate gradation shows optimum compressive strength of the order of 8.6, 15.9, and 17 MPa at 7, 28 and 56 days of curing. Furthermore, the visual inspection test shows that clogging by clay clogger shows an even distribution of sediment on the whole length of the sample.

KEY WORDS: Pervious concrete; Permeability; Porosity; Compressive strength; Clogging potential.

Citation/Citar como: Nazeer, M.; Kapoor, K.; Singh S.P. (2023) Experimental investigation of clogging mechanism of pervious concrete made with variable aggregate gradations. Mater. Construcc. 73 [351], e320. https://doi.org/10.3989/mc.2023.319922.

RESUMEN: *Investigación experimental del mecanismo de obstrucción del hormigón permeable hecho con gradaciones variables de áridos.* En este estudio se evaluó el mecanismo de obstrucción del hormigón permeable utilizando tres obturadores diferentes: arena (S), arcilla (C) y una combinación de arena y arcilla (S & C). El mecanismo de taponamiento se realizó a través de un aparato de permeabilidad de cabeza descendente, utilizando una carga de sedimento del obturador a razón de 50, 150 y 200 gramos en ciclos de taponamiento repetitivos. A partir de los resultados se observó que el obturador combinado (S & C) muestra resultados críticos generales de obstrucción, ya que el 80% de la obstrucción se observó de 3 a 4 ciclos. Además, se detectó que la mezcla de hormigón permeable hecha con gradación de áridos tipo R presenta una resistencia a la compresión óptima del orden de 8.6, 15.9 y 17 MPa a los 7, 28 y 56 días de curado. Finalmente, la prueba de inspección visual muestra que la obstrucción por arcilla muestra una distribución uniforme de sedimentos en toda la longitud de la muestra.

PALABRAS CLAVE: Hormigón permeable; Permeabilidad; Porosidad; Resistencia a la compresión; Potencial de obstrucción.

1. INTRODUCTION

According to ACI, Pervious Concrete is a highly porous concrete that can be used combinedly as a pavement and drainage system. In recent times, pervious concrete has been the most significant development in concrete technology and had a profound environmental benefit. It is a special type of concrete made with or without the inclusion of fine aggregate content than a normal conventional type of concrete. It is widely used in pedestrian footpaths, car parks, sidewalks, car washing areas, efficient sanitization systems, and slope stability in hilly areas and other low-traffic areas (1–4). Pervious concrete provides many advantages when used as pavement material, it recharges the groundwater, and it eliminates the need for a 2 to 3% slope to prevent ponding (5). It minimizes the heat island effect (6–9). Moreover, pervious concrete as pavement material generates less noise from traffic and low thermal conduction as compared to asphalt or conventional rigid pavement (10, 11). For its diverse environmental benefits, it was also tagged as the best stormwater mechanism by Environmental Protection Agency (EPA) and Low Impact Development (LID) system (12–14). As per reports of ACI, the normal size of pores in pervious concrete fluctuates between 2-4 mm and it may vary due to several aspects such as powder to aggregate ratio, water to cement ratio, and size and shape of aggregates (15–17).

Moreover, the porosity of pervious concrete ranges between 15% to 30% (18, 19). However, there is serious concern that due to high turbid runoffs containing fine silt, sand, and clay and frequent erosion of organic and inorganic fine particles from surroundings, temporary chocking of pervious concrete pavement. This temporary accumulation of these fine materials inside the pores leads to the clogging of pavement made with pervious concrete (20–22)**.** Therefore, the efficacy of pervious concrete when used as pavement decreases due to diminishing hydraulic permeability (23). Thus, the problem of serviceability and premature degradation starts at an early age and cuts the service life of pervious concrete pavement. When a significant percentage of pores in the pervious concrete pavement gets clogged, water starts pooling on the surface and causes waterlogging of pervious concrete pavement. Moreover, the standing water over the road surface for a long time accelerates the deterioration of the pervious concrete pavement and sometimes causes unpleasant nuisance and water-borne diseases (24–27). However, a small amount of research is available on averting the clogging problems in pervious concrete pavement systems. Different maintenance and rejuvenation techniques such as vacuuming, pressure washing, and sweeping have been adopted (28–30). However, all these techniques show limited results as these were effective only to a depth of 15- 20 mm (31).

Some authors have investigated surface cleaning with pressurized water and air-blowing techniques and suggested that the air-blowing technique is the best practice to de-clog the choking (32). Others have investigated that the combined effect of sand and clay produces a flash downfall in permeability as seen for single loaded sediment such as single sand or single clay cycle of runoff, however, complete blocking of pores was seen between 2 to 13 cycles of artificial runoff (33). Gersson studied the effect of fine sediments over the clogging of pervious concrete and found that fine sediment is more damaging for a reduction in hydraulic conductivity due to the smaller size of sediments (34). Haselbach performed the clogging of pervious concrete using clay sediments and found that the rate of clogging depends on the density of rinsing runoff. Moreover, it was observed that less cohesive sediments can be removed easily by applying sweeping as compared to more cohesive soils (35). Alalea Kia found the critical condition of clogging happens due to choking of top surface pores and traveling of fine particles to the lower strata of samples. It was also mentioned that all the rehabilitation techniques reestablish the permeation volume partially and rehabilitation cannot work if choking happens a few centimeters below the top surface of pervious concrete (36).

2. RESEARCH SIGNIFICANCE

Based on the literature survey presented in the preceding section indicates that a lot of research has been done to examine the strength and hydraulic properties of pervious concrete made with single grade proportion of aggregates. However, the information on clogging potential for pervious concrete made with different aggregate grade proportions is scanty. Therefore, an investigation has been developed on the effect of grade aggregate proportions on the clogging phenomenon of pervious concrete. In this study, three grades proportion of aggregates (P, Q, and R) were prepared from four aggregates proportions (A: B: C: D) such as 2.36 mm, 4.75 mm, 6.3 mm, and 10 mm. Moreover, to stimulate the actual sediment load conditions and to calculate actual load percentages, sieve and hydrometer analyses have also been done. Furthermore, other properties such as porosity, permeability, and compressive strength have been evaluated at 28 and 56 days of curing. Additionally, a visual inspection test through the half-cut method, dry cut method, and slicing method is performed to check the flow and depth of clogging sediment.

3. EXPERIMENTAL PROGRAMME

The experimental program in this study was divided into two general findings. The first aim involves the determination of porosity, water permeability, and compressive strength. secondly, the clogging perfor-

mance of pervious concrete was evaluated using three different sediment cloggers.

3.1. Materials

The different materials utilized in this experimental study have been discussed in the following sub-sections.

3.1.1. Cement

Ordinary Portland Cement (OPC) 43 grade, according to IS: 8112 (37) was used as a primary binder. The consistency was 32.5%, and the fineness of 6% was determined as material properties in the present investigation as per guidelines of IS 4031 (Part 2 and 4) (38, 39). The physical properties such as specific gravity (3.15), initial setting time (40 minutes) and final setting time (240 minutes) were also determined as preliminary testing of OPC binder.

3.1.2. Aggregates

The three different grades (P, Q, and R) of Natural Coarse Aggregates (NCA) and Natural Fine Aggregates (NFA) have a size of 12-10 mm, 10-6.3 mm, 6.3-4.75 mm, and 4.75-2.36 mm were used in the ratio of A:B:C:D. The different grades were used in the ratios of, 0:40:40:20, (i,e 0% of 2.36 mm, 40% of 4.75 mm, 40% of 6.3 mm, and 20% of 10 mm) for P, 10:40:40:10 (i,e 10% of 2.36 mm, 40% of 4.75 mm, 40% of 6.3 mm, and 10% of 10 mm) for Q, and 20:40:40:0 (i,e 20% of 2.36 mm, 40% of 4.75 mm, 40% of 6.3 mm, and 0% of 10 mm) for R, respectively. Natural Fine Aggregates, 2.36 mm was obtained locally and was utilized in the ratios of 0%, 10%, and 20% as per IS 383 guidelines (40). The particle distribution for all three grades (P, Q, and R) is plotted as per IS 2386 (part 1) (41) and presented in Figure 1.
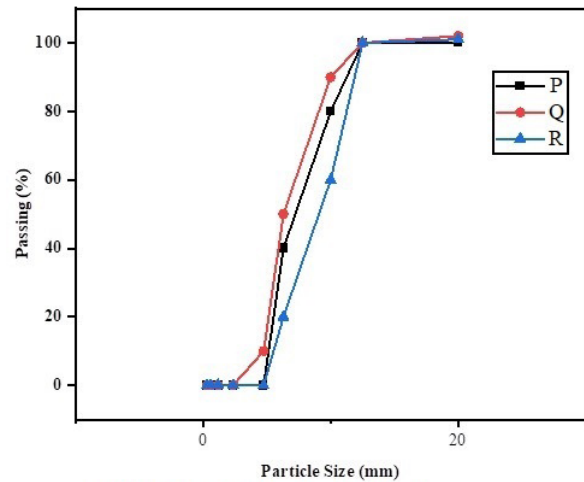

FIGURE 1. Particle size distribution curves.

Moreover, the different physical properties and their standards are presented in Table 1.

3.1.3. Sediment load

Sediment load for clogging was selected from the actual road dust sample and the particle size distribution is shown in Figure 2. It was seen from the results of the hydrometer that 70% of particles present in finer dust were clay and only 30% were silt. The loading rate of sediments used in this study was of the order of 50 grams of fine sand, 150 grams of kaolin clay, and 200 grams of sand and clay in combination were used as for sand (S), clay (C), and Combined "Sand & clay" (S & C) respectively.

3.2. PC mix proportions

The mix proportions of the different pervious concrete mixes are presented in Table 2. All the quantities

TABLE 1. Physical properties of aggregates and testing standards.

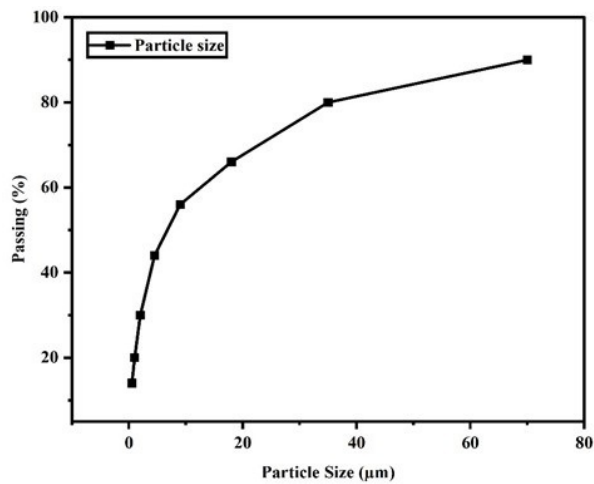| Aggregate properties	2.36 mm (NFA)	4.75 mm (NCA)	6.3 mm (NCA)	10 mm (NCA)	Testing standards
Impact value (%)	-	13.36	13.10	13.00	IS:2386-Part-IV (53)
Abrasion value (%)	-	20.86	19.00	18.03	ASTM C 131 (54)
Water absorption (%)	2.10	0.56	0.57	0.98	ASTM C127 (55)
Soundness (%)	-	5.70	5.68	5.30	IS:2386-Part-V (56)
Apparent density (kg/m³)	2490	2445	2420	2410	ASTM C127 – 15 (57)
Bulk density (kg/m³)	1795	1780	1765	1750	ASTM C29/C29M (58)

Figure 2. Particle size distribution of road dust.

(cement and aggregates) are measured by taking the overall unit weight of pervious concrete as 1920 kg/m³. The basic mix proportions for all the mixes were taken following ACI-522R-s2010 (42). The pervious concrete mixes were made using a tilting drum mixer in the lab at the authors' institute as shown in Figure 3. A sufficient number of specimens were cast to conduct all the tests for this study. Cylindrical samples (100×200 mm) were cast for porosity, permeability,

and clogging. However, for compressive strength testing, cubes measuring 150 mm in size were cast.

3.3. Test methods

After 24 hours of casting, the specimen was demoulded and placed in a curing tank for 7, 28, and 56 days at room temperature conditions (20 ± 1°C while as humidity was maintained over 95%. All the testing procedures are discussed in the following sub-sections.

3.3.1. Porosity

ASTM C1754 (2012) was used to evaluate the porosity of the pervious concrete (43). The initial mass of the sample is taken in submerged condition as W_1. The sample was then dried in an oven for 24 hours at 105 °C, and the dry mass of the sample in the air was taken as W_2. The porosity of three samples from each batch of pervious concrete was taken and the final porosity was calculated as the average of the three values. The porosity (P) was calculated using Equation [1].

$$P = \left[1 - \frac{(W_1 - W_2)}{V \rho_w}\right] \times 100\% \qquad [1]$$

Figure 3. Drum mixer and output of mixer.

Table 2. Mix proportions of pervious concrete.

Mix Notation	Aggregate proportion (AP)	AP Notation	W/C ratio	P/A ratio	2.36 mm (A)	4.75 mm (B)	6.3 mm (C)	10 mm (D)	OPC Kg/m³	Water Kg/m³
P-A0	0%A+40%B+40%C+20%D	P	0.35	1:5	0	640	640	320	320	112
P-A10	10%A+40%B+40%C+10%D	Q	0.35	1:5	160	640	640	160	320	112
P-A20	20%A+40%B+40%C+0%D	R	0.35	1:5	320	640	640	0	320	112

Where P is the porosity of cylindrical sample, %; W_1 is the mass of sample in dry condition, g; W_2 is the mass of sample in submerged condition, g; V represents volume specimen, cm³; and ρw represents the density of water, g/cm³.

3.3.2. Permeability

A falling head permeability apparatus as shown in Figure 4, was used to measure the permeability of pervious concrete. A cylindrical sample is fitted inside the black collar and a water head of 90 cm is maintained in a graduated PVC tube. A fabric inch tape and thin transparent pipe also adhere for head reading and piezometer purposes respectively. To ensure that the pervious concrete sample is saturated, valve (v_1) is kept open initially and a trial is performed between a preliminary head (h_1) of 90 cm and a bottom head (h_2) of 30 cm. As the sample is saturated fully, the permeability test is performed by calculating the time (t) that it took from head (h_1) to head (h_2) using a stopwatch. Finally, the permeability was calculated using Darcy's Equation [2].

$$K = (A_1/A_2)\frac{L}{t}\ ln(h_1/h_2) \qquad [2]$$

Where K is permeability, A_1 is the area of the head pipe, A_2 is the specimen area, L is specimen length and 't' is the time required for water to drop from the preliminary head h_1 to bottom head h_2.
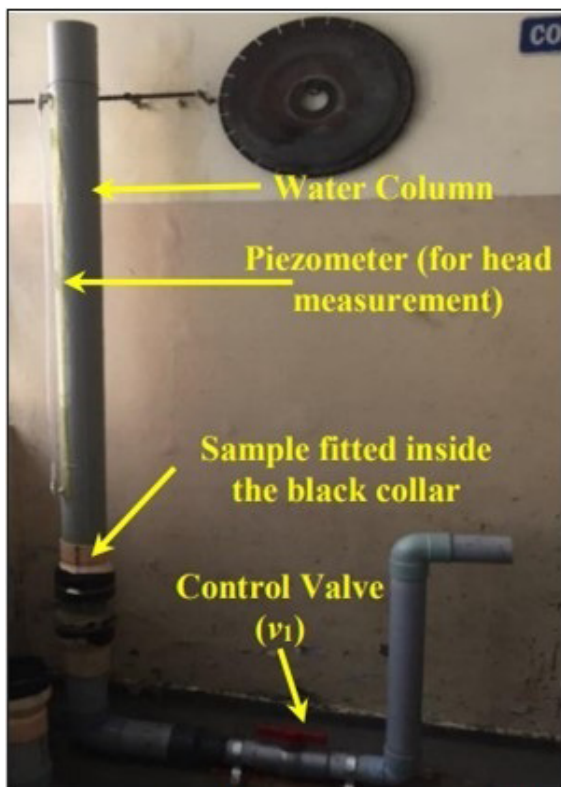

FIGURE 4. Falling head permeability apparatus.

3.3.3. Compressive strength

A compressive strength test on pervious concrete was performed according to IS 516 (1959), (44). A compression testing machine with a 2000 kN maximum loading capability was used to perform the compressive strength test of pervious concrete. A sample size of 150 mm cube was loaded till failure at a rate of 5.2 kN/sec.

3.3.4. Clogging potential

3.3.4.1. Permeability reduction

The falling head permeability apparatus used for measurement of permeability was used to evaluate the outcome of artificial clogging in pervious concrete. Three cloggers (S, C, and S&C) were used to produce artificial runoff and permeability reductions are calculated using Darcy's Equation [2].

3.3.4.2. Visual observation of clogging

To know whether the blockage in the pore channel was at the top, bottom, or center, a visual inspection is necessary to perform. In this study visual inspection was performed through three techniques. a) Half-cut method: In this method, the clogged samples of pervious concrete are cut into two halves as shown in Figure 5 and the weight of each half is taken. It provides an idea of whether cloggers are present only on the top surface half or on the lower half. b) Dry cut method: It is a visual inspection in which a clogged sample is transversely cut into two halves as shown in Figure 6 to know the location of sediments inside the clogged sample. The sample is cut under CTM using upper and lower steel strips. C) Slicing method: Diamond saw cutter is used to cut the clogged sample into four halves as sown in Figure 7 to know the distribution and tortuosity of sediment flow.

3.3.4.3. Image Processing of clogging

With the help of a high-resolution micro-focus X-ray computed tomography (X-CT) system and filter 7 image processing software, the exact presence of sediment was predicted with clear visuals. Moreover, the clogging of clogged sample was predicted through X-CT at three sections, top, mid, and bottom respectively.

3.3.4.4. Rejuvenation of clogging

Two rejuvenation techniques are used to un-clog the clogged samples of pervious concrete are:
a. Vacuum rejuvenation
b. Pressure washing

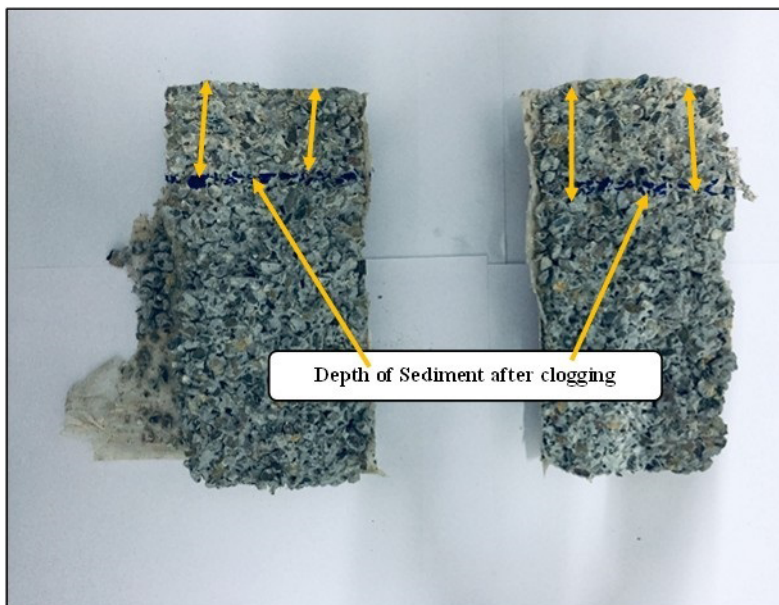**FIGURE 5.** Half cut method of clogged sample.

FIGURE 6. Dry cut method of clogged sample.

FIGURE 7. Slicing method of clogged sample.

Eureka Forbes vacuum cleaner having a suction capacity of 2300 mm of WC (0.022 MPa) was used for vacuum treatment of clogging. Both the nozzles, floor cum carpet, and crevice nozzle were used to remove the sediment particles from cylindrical samples. Whereas, a car service pressure washer having 20.7 MPa (3,000 psi) pressure of water was used pressure washing treatment of clogging. Both the rejuvenation methods are intended to wash out the ingressed materials and regain the hydraulic functionality of clogged pervious concrete samples.

4. EXPERIMENTAL RESULTS AND DISCUSSION

4.1. Porosity

The porosity of all the mixes of pervious concrete made with different grade aggregate proportions is presented in Figure 8. Porosity obtained in this study was in the range of 18 - 20% which is in the qualified range of results observed in the literature (15-35%) (45–48). It was observed from the results that porosity of pervious concrete across all the curing ages decreases marginally with changing the aggregate grade proportion from P to R. For example, in the mix P-A10, in which aggregate gradation Q was used having 10% of NFA content, relative to pervious concrete control mix, P-A0 having 0% NFA, the reduction in the porosity was 3% and 2.5% at 7 and 28 days respectively, which is significant. However, for the mix containing R type of aggregate gradation in which 20% of NFA was included, I,e mix P-A20, the porosity reduction relative to control mix P-A0 at the curing age of 7 and 28 days was 8% and 10.25% respectively. The behavior is similar to that observed in pervious concrete where similar reductions in porosity have been reported in literature upon the inclusion of NFA with NCA (49, 50). It is obvious that porosity is a volumetric property, therefore the volume of the void will depend upon a few parameters like the size of aggregates, the proportion of fines, the amount of binder content, etc. Generally, the pervious concrete prepared with a higher p/a ratio had lower porosity due to the reduction of cement content than the mix prepared with a lower p/a ratio. The increase in cement content increases the packing density of the matrix, thereby reducing the porosity of pervious concrete. Similarly, the effect of aggregate gradation has the same effects on porosity that as the amount of fine content is increased porosity decreases due to an increase in apparent density of pervious concrete. The apparent density of mix containing 0% of NFA (I, e mix P-A0) was 1960 kg/m^3, while as the mix containing 10% and 20% of NFA have the apparent densities of the order of 1984 kg/m^3 and 2009 kg/m^3 respectively, which is 1.2% and 2.5% higher than

the control mix. Therefore, with increasing the values of apparent densities, porosity of pervious concrete decreases significantly.
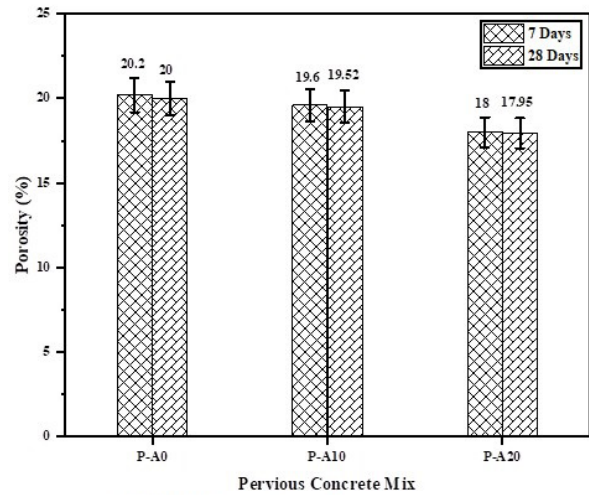
FIGURE 8. Porosity of pervious concrete.

Furthermore, it was also observed from Figure 8 that at two different curing ages, a marginal decrease in the porosity of pervious concrete was seen. On comparing porosities of mix P-A0 at 7 and 28 days, a borderline decrease of 1% was seen at 28 days age of curing as compared to porosity seen at 7 days. This marginal decline in porosity after 28 days was due to further strength gain due to which the micropores of paste get filled and a marginal reduction in porosity is observed. Similarly, for mixes P-A10 and P-A20, a small decrease in the porosity of pervious concrete at 7 and 28 days was observed. A decrement of 0.5% and 0.3% in porosity of mix P-A10 and P-A20 respectively was seen at 28 days as compared to porosity observed at 7 days of curing age.

4.2. Permeability

The water permeability tests on pervious concrete were performed at 7 and 28 days of curing age and are presented in Figure 9. Here we assume the meaning of PC conferring to the American Concrete Institute which mentions the working range of permeability coefficient from 0.13-1.2 cm/s (51). It can be seen from Figure 9 that pervious concrete shows a declinement in permeability with the change in aggregate grade proportion from P to R. A maximum permeability of 0.92 cm/s was seen for control mix P-A0, in which aggregate grade proportion R was used, having 0% NFA content. A significant decrease in permeability was seen for mix P-A10, in which Q type aggregate grade proportion was included, having 20% NFA. For mix P-A10, a decrease of 4.5% and 5% at 7 and 28 days of curing was observed as compared to

control mix P-A0, which is a significant drop. Moreover, for mix P-A20, in which R type aggregate grade proportion was used having 20% content of NFA as compared to control mix P-A0. A significant drop in permeability of pervious concrete was observed at 22% and 23% at the curing ages of 7 days and 28 days as compared to the permeability of control mix P-A0. It was further observed from the results of permeability that a marginal drop in permeability was seen for all the mixes of pervious concrete after 28 days of curing. For example, for the control mix, P-A0, in which the NFA percentage was 0%, a reduction of 0.5% was seen at 28 days as related to 7 days. Moreover, a reduction of 0.5% and 1% in permeability was seen for mix P-A10 and P-A20 respectively after 28 days of curing as compared to 7 days of permeability. This marginal drop in permeability at 28 days of curing was due to the development in the microstructure of pervious concrete which is also confirmed by enhancement in compressive strength after 28 days of curing. Therefore, readjustment of micropores is seen at higher curing age due to which permeability drop is seen.
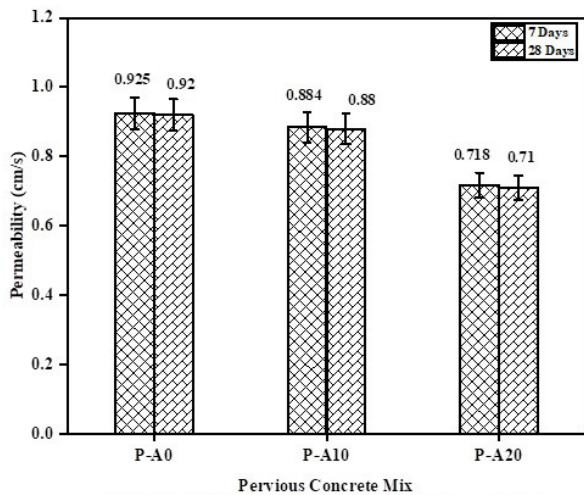

FIGURE 9. Permeability of pervious concrete.

Furthermore, a relationship was developed between permeability and porosity of all the mixes as shown in Figure 10. It was observed from the relation that R^2 holds a decent range of 0.9. Therefore, the permeability of pervious concrete can be projected from the initially calculated porosity.

4.3. Compressive strength

The compressive strength results of the pervious concrete mixes made with three aggregate grade proportions are presented in Figure 11 which shows that the compressive strength of all the mixes increases significantly with changing the aggregate grade proportions from P to R. For example, significant devel-
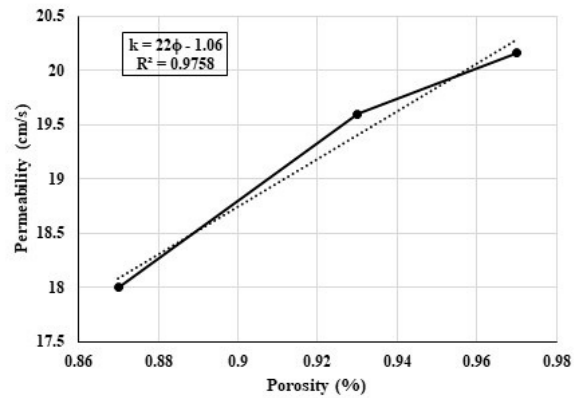

FIGURE 10. Relationship between permeability and porosity.

opment of 8%, 10% and 3% in compressive strength was seen for mix P-A10 in which Q series of aggregate grade proportion was used at curing age of 7, 28 and 56 days, relative to mix P-A0, which is control mix. The significant development in the results of compressive strength at all the curing ages was due to the inclusion of 10% of NFA in the Q series of aggregate proportion, thereby due to which the development in paste density magnifies the results of compressive strength. However, for the mix containing R type series of aggregates having 20% NFA content I, e mix P-A20, the strength development relative to controller mix at 7, 28, and 56 days was 21%, 24%, and 15%, which is more prominent. A similar trend in the development of compressive strength has been reported in the literature that due to substitution of a fine up to 5% increases the mechanical strength of pervious concrete (52). The significant increment in compressive strength with incorporation of different percentages of NFA was due to the overall development in apparent density of pervious concrete. It was observed from the results that with incorporation of 10% of NFA, apparent density of pervious concrete increases by 1.2% relative to mix containing 0% of NFA. Moreover, a maximum increment of 2.5% in apparent density of pervious concrete can be seen for mix containing 20% of NFA relative to P-A0, containing 0% of NFA. Therefore, with increasing the apparent density of pervious concrete, compressive strength increases significantly.

Furthermore, the development of compressive strength in pervious concrete shows optimum results at 28 days of curing for each mix as compared to the compressive strength of pervious concrete at 7 and 56 days. A prominent development of 43% in compressive strength was seen for the control mix, at 28 days as compared to 7 days strength. Nevertheless, the increase in strength for the same control mix, P-A0 at 56 days was only 17% as compared to compressive strength at 28 days. Moreover, the same increment in compressive strength for pervious concrete was seen for mix P-A10 and P-A20, in which aggregate grade proportion of Q and R type was used having 10%
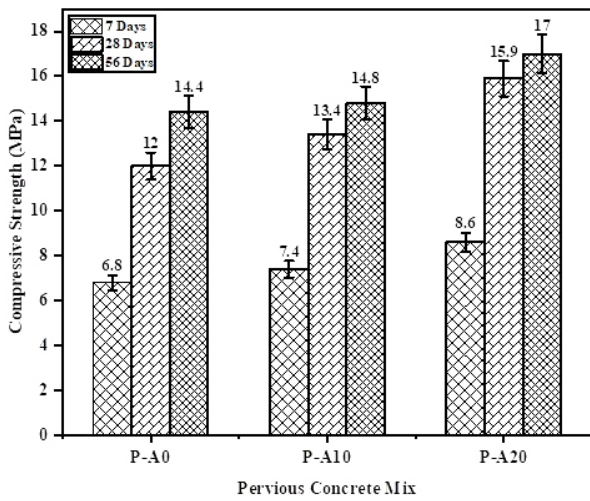
FIGURE 11. Compressive strength results of pervious concrete.

and 20% of NFA respectively. An increment of 45% and 46% was observed for mix P-A10 and P-A20 at 28 days as compared to compressive strength at 7 days. However, a marginal development of 9% and 6% in compressive strength was seen for the same mixes of P-A10 and P-A20 at 56 days as compared to compressive strength at 28 days. This shows that on increasing the curing period from 7 to 28 days, maximum hydration of pervious concrete mix occurs at 28 days because of higher creation of C-S-H which contributes to more compressive strength. The increase in strength was also attributed to the more pozzolanic and filler effect of pervious concrete by incorporating more NFA which increases the overall density of pervious concrete. For pervious concrete mix in the varied graded proportion of aggregates.

4.4. Clogging of pervious concrete

4.4.1. Permeability reduction

The falling head permeability apparatus used for measurement of permeability was used to evaluate the outcome of artificial clogging in pervious concrete as shown in Figure 12. The test was started by calculating the initial permeability of pervious concrete without any sediment load which acts as reference permeability. As the preliminary permeability was calculated, dry sediment was progressively added evenly to the top surface of the specimen before adding extra water to simulate the clogging phenomenon. It can be seen from Figure 13 (a) that the permeability of each sample reduces after each cycle of runoff. For the control mix, P-A0, the initial average permeability was 0.92 cm/s and it starts declining as compared to initial permeability after progressive sand-laden runoff cycles as 7.6%, 23%, 36%, 58%, 71%, 86%, 92%, 94% and 100% for 10 cycles in total, however, the working limit of permeability ends at the 7th cycle where clogging was almost 80% and remaining permeability of sample was only 0.12 cm/s. For the same control mix, on applying the clay-laden runoff, permeability declinement was more gradual than sand-laden runoff. The reduction percentage of permeability was 3%, 7%, 20%, 41%, 60%, 75% 85%, 95%, and 100% for 9 cycles. However, 80% of clogging was done after the 7th cycle at which the remaining permeability of pervious concrete was below the permissible limits. Moreover, for the same mix, combined (S and C) laden runoff shows a quick declinement in permeability. The decrease in permeability was seen at 38%, 55%, 70%, 85%, 97% and 100% for 6 cycles of combined
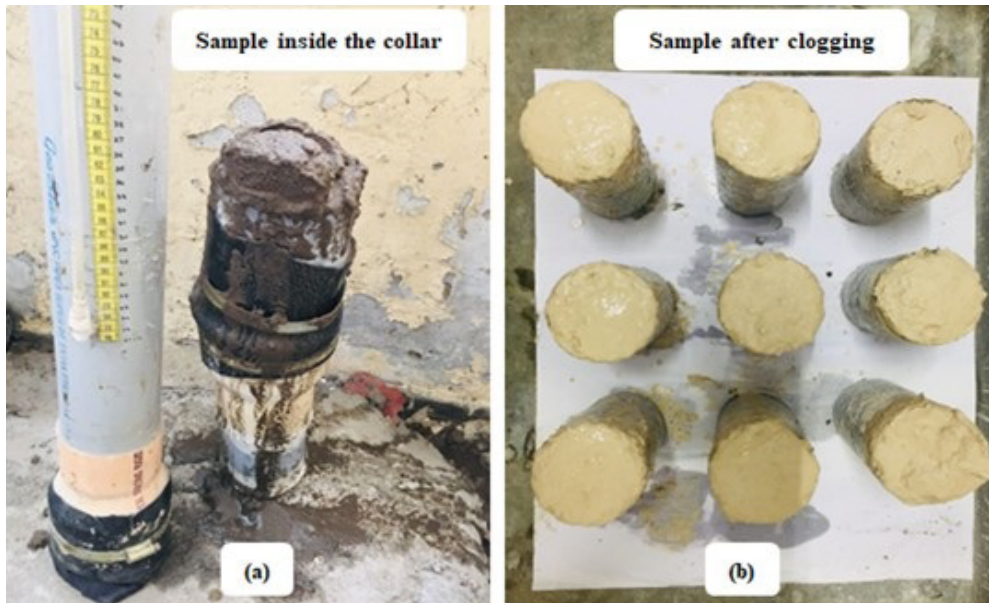

FIGURE 12. Clogged samples: (a) sand clogging; (b) clay clogging.

sand and clay runoff. Moreover, the permissible limit of permeability was crossed in the early 4th cycle of runoff at which 85% of clogging was seen. This quick declinement in permeability for the combined laden runoff was due to the formation of a mud lid over the surface of the sample. Therefore, flocking of clay with fine sand particles causes early blocking of surface pores of pervious concrete by forces of Van der Waals.

From Figure 13 (b) the initial average permeability for mix P-A10 was 0.90 cm/s and it starts declining after progressive sand-laden runoff cycles as compared to initial permeability of 14%, 20%, 33%, 46%, 58%, 70%, 82%, 93% and 100% for 9 cycles in total, however, the working limit of permeability ends at the 7th cycle where clogging was almost 82% and remaining permeability of sample was only 0.12 cm/s. For the same control mix, on applying the clay-laden runoffs, permeability declinement was more gradual than

sand-laden runoff. The reduction percentage of permeability was 4%, 12%, 24%, 41%, 57%, 69% 80%, 86%, 94% and 100% for 10 cycles. However, 80% of clogging was done after the 7th cycle at which the remaining permeability of pervious concrete was below the permissible limits. Moreover, for the same mix, combined (S and C) laden runoff shows early clogging in pervious concrete. The decrease in permeability when compared to initial permeability was seen as 32%, 52%, 66%, 74%, 86% and 93%, 98%, and 100% for 8 cycles of combined sand and clay runoff. Moreover, the permissible limit of permeability was crossed at the early 5th cycle of runoff at which 86% of clogging was observed. Furthermore, the reduction in permeability for mix P-A20 was faster as compared to previous mixes due to low porosity (18%) as shown in Figure 13 (c). Moreover, 80% clogging in pervious concrete occurs at the 5th, 6th, and 3rd cycle after performing sand, clay, and combined runoff cycles respectively. However, the
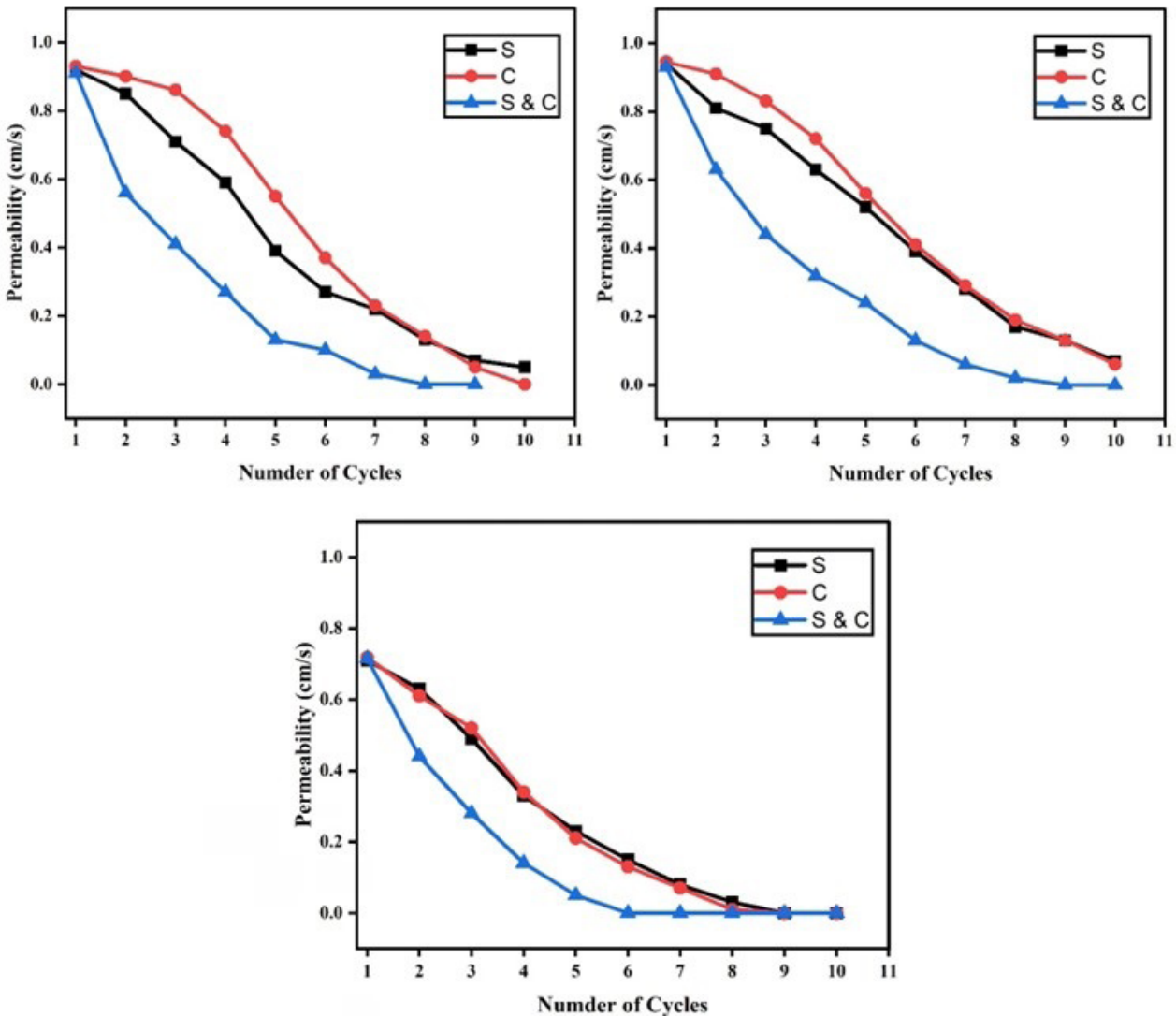

FIGURE 13. Clogging of pervious concrete for mix a) P-A0, b) P-A10, and c) P-A20.

complete (100%) clogging of pervious concrete occurs on the 7th, 8th, and 5th for sand, clay, and combined run-off laden.

4.4.2. Visual observation of clogging

It can be seen from Figure 13 that the permeability of pervious concrete was initially highest but decreased exponentially due to the choking of pores. However, the exact reason for the blockage of pores was observed from visual inspection. It was observed from the half-cut method of clogging that samples clogged with fine sand show a significant weight difference between the upper half and lower half. From the results it was observed that the upper half weight for the sand clogged sample was more than the lower half, indicating that major sediment was accumulated on the upper half of pervious concrete. Moreover, no weight difference was seen in samples clogged with clay, as it was observed from the dry cut method that clay sediment was seen evenly through the whole depth of the sample. Moreover, the samples clogged with both sand and clay showed a clear presence of sediment only on the upper top 5 cm, which was also confirmed from the half-weight method of pervious concrete.

It was also analyzed from the slicing method of visual inspection that the clay clogger was evenly distributed over the whole length of the sample. However, peripheral sand sediment was seen at the outer periphery of cylindrical samples clogged with sand only as shown in Figure 14. It indicates that sandy clogger flows with water through the shortest radial flow path. Therefore, in general, it can be concluded that clogging due to clay is critical because of its cohesive nature, makes a strong bond inside the pores, and is difficult to unclog through rehabilitation techniques.
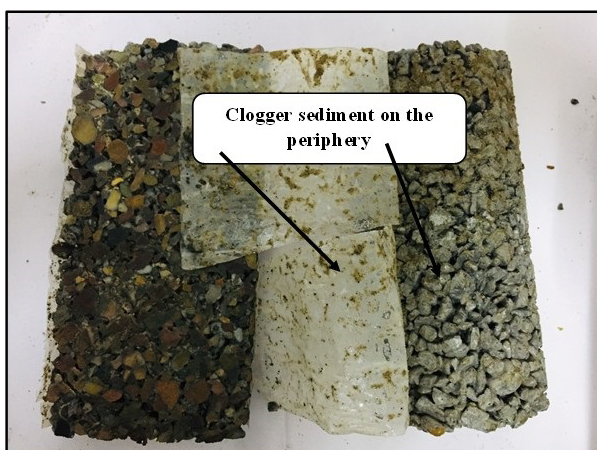

FIGURE 14. Peripheral sediment in sand clogging.

4.4.3. Image processing of clogging

The image processing techniques such as X-CT tomography and filter 7 image processing were used

and are shown in Figure 15 and Figure 16. To know the actual depth of sediment, X-CT tomography of clogged cylindrical sample was performed at three different sections (top, mid, and bottom). A 200 mm cylinder was cut into three equal discs and X-CT of each 65 mm disc was performed separately. It can be seen from Figure 15 (a) that distribution of sediment particles for sand clogged sample were more on the top section of the sample. The intensity of sediment particles for the sample starts decreasing with the depth of sample. Therefore, it confirms the visual examination of above section that sand sediment flows through shortest outer periphery path. Moreover, X-CT of cylindrical sample clogged with clay alone as seen in Figure 15 (b), shows that distribution of clay particles was seen evenly throughout the depth of sample. It can be further seen from the same tomography that clay particles predominantly clinged with each other with the help of weak vander waals forces due to sticky nature. Furthermore, the tomography of cylindrical sample clogged with combined sediment load shows that sediment was only present on the top section of clogged sample. Therefore, with the variable charged particles of sand and clay, a mud lid was formed on the top of sample shows that choking of voids is only to the top section of pervious concrete. Therefore, clogging with clay shows chocking through all the over the depth, which could be more severe and critical. Moreover, image processing filter 7 was used to counter check the presence of clay sediment which is considered to be more critical. It can be seen from Figure 16 that distribution of sediment load was evenly distributed over the whole depth of sample, which is in full agreement with the above study of tomography technique.

4.4.3.1. Rejuvenation of clogging

Vacuuming as shown in Figure 17 was performed on all the mixes of pervious concrete through carpet and crevice nozzle for a minute after drying the sample in the oven for 24 hours at 60 °C. It was observed from the results of this treatment that sand clogged sample shows a maximum recovery of 80% regain in permeability. Moreover, a worst rate of recovery of the order of 10% was observed for the samples clogged with clay alone. Whereas, recovery against combined (S & C) clogger was observed as 40%. However, aggregate pervious concrete mix combination made with P-type of aggregate gradation shows optimum results against both the rejuvenation techniques relative to other mix combinations made with Q, and R-type of aggregate gradations. This optimum recovery for P-type of mix combination could be due to higher porosity relative to other mix combinations. Vacuuming extracts, the ingressed material of clogging from the sample, therefore mix having more voids enables large suction cavity through maximum depth of sample.
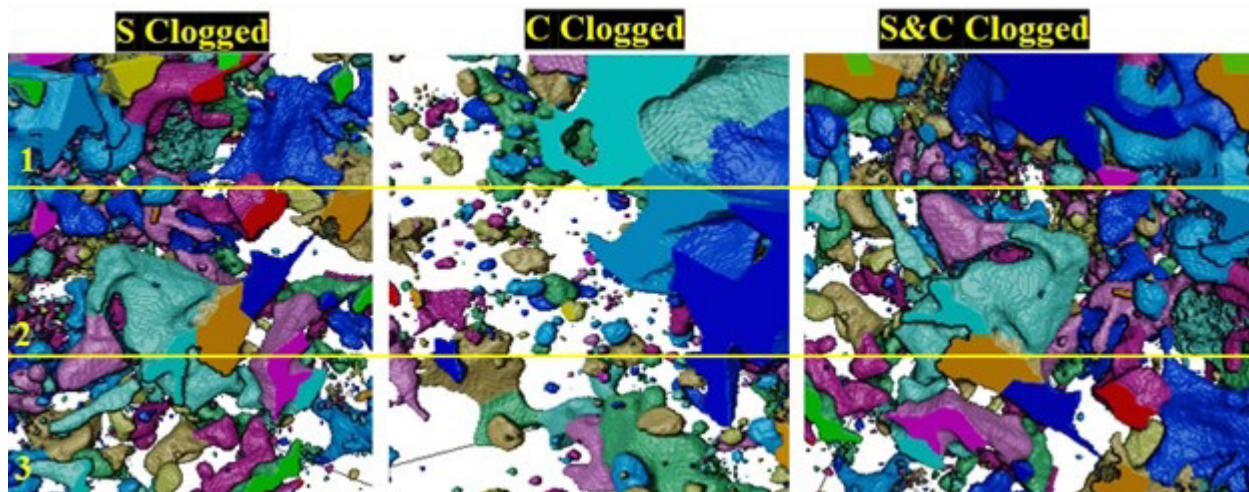
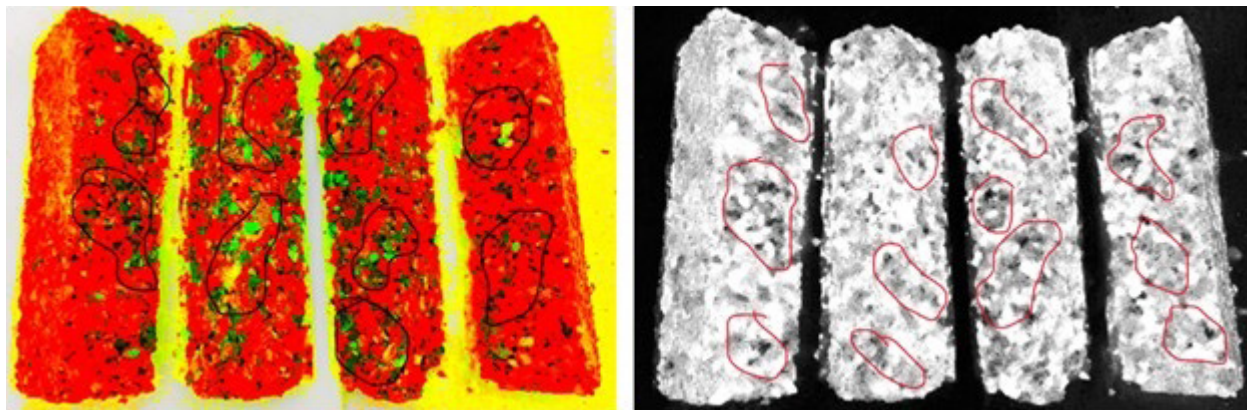**Figure 15.** C-T of clogged specimen of pervious concrete.

Figure 16. Image processing of clogged specimen of pervious concrete.

Figure 17. Rejuvenation of clogged specimen of pervious concrete.

Moreover, pressure washing as shown in Figure 17 (a) pushes out or washes the impurities through the pervious concrete sample. A maximum recovery of pressure 50% was seen for samples clogged with combined (S&C) clogger sediment. This could be possible that combined sediment forms the mud lid over the top surface of sample, which stops maximum amount of sediment on the top surface without blocking the internal path of voids. However, results of pressure washing against sand shows worst results (20% recovery) due to secondary clogging of lower section. Due to pressure washing sand particles easily move down the top section of sample and settles in the lower section of sample. However, using pressure washing in the opposite direction for the same sample shows some development in de-clogging but the development was marginal. Furthermore, pressure washing against clay clogged shows a recovery rate of 30%, which is acceptable. Pressure washing dissolves some loose part of clay and drains out on the other side of sample. It was further, observed that the overall recovery of pressure washing was optimum for mix combinations made with R-type of aggregate gradation due to higher ranges of porosity relative to other combinations of pervious concrete.

5. CONCLUSIONS

The present study was designed to determine the influence of different aggregate grade proportions on the clogging potential of pervious concrete. Based on the results obtained, a few conclusions are drawn.

1. Relative to the control mix, made with P-type of aggregate gradation, the 28-day compressive strength increased significantly by 10% and 24% for mixes P-A10 and P-A20 in which Q and R type aggregate grade proportion was used respectively. Therefore, the inclusion of NFA up to 20% in pervious concrete increases the compressive strength significantly at 28 days of curing age due to increasing the overall density of concrete matrix.
2. Clogging done by combined sand and clay clogger shows an 80% loss in permeability in 4 to 5 cycles for all three mixes. However, clogging through clay alone take highest number of cycles (9-10) to reach 80% of clogging, therefore could show worst case of clogging due to even filling of pores through whole length of sample.
3. All the visual observations supported by image processing shows that clogging due to clay alone could show critical results of clogging as the sediment of clay was evenly distributed over the whole depth of sample. Whereas, clogging due to combined sediment shows least clogging due to formation of mud lid on the top of sample.
4. Rejuvenation treatment shows that a maximum 80% recovery of permeability was observed for

sand clogged samples against vacuuming treatment. Whereas, a maximum recovery of 50% in permeability was seen for combined clogged samples against pressure washing. However, in general it was observed that pervious concrete mix made with R-type of aggregate gradation shows optimum results of recovery against both the rejuvenation techniques.

AUTHOR CONTRIBUTIONS:

Conceptualization: K. Kapoor, S.P. Singh. Data curation: K. Kapoor, M. Nazeer. Formal analysis: K. Kapoor, S.P. Singh, M. Nazeer. Investigation: K. Kapoor, M. Nazeer. Methodology: K. Kapoor, S.P. Singh, M. Nazeer. Project administration: K. Kapoor, S.P. Singh. Resources: K. Kapoor, S.P. Singh. Supervision: K. Kapoor, S.P. Singh. Validation: K. Kapoor, S.P. Singh, M. Nazeer. Visualization: K. Kapoor, S.P. Singh, M. Nazeer. Writing, original draft: M. Nazeer. Writing, review & editing: K. Kapoor, S.P. Singh.

REFERENCES

1. Wang, H.; Li, H.; Liang, X.; Zhou, H.; Xie, N.; Dai, Z. (2019) Investigation on the mechanical properties and environmental impacts of pervious concrete containing fly ash based on the cement-aggregate ratio. *Constr. Build. Mater.* 202, 387–95. https://doi.org/10.1016/j.conbuildmat.2019.01.044.
2. Nguyen, D.H.; Boutouil, M.; Sebaibi, N.; Baraud, F.; Leleyter, L. (2017) Durability of pervious concrete using crushed seashells. *Constr. Build. Mater.* 135, 137–50. https://doi.org/10.1016/j.conbuildmat.2016.12.219.
3. Calkins, J.; Kney, A.; Suleiman, M.T.; Weidner, A. (2010) Removal of heavy metals using pervious concrete material. *World Environ. Wat. Res. Cong.* 37, 74–83.
4. Gaedicke, C.; Marines, A.; Miankodila, F. (2014) A method for comparing cores and cast cylinders in virgin and recycled aggregate pervious concrete. *Constr. Build. Mater.* 52, 494–503. https://doi.org/10.1016/j.conbuildmat.2013.11.043.
5. Ali, T.K.M.; Hilal, N.; Faraj, R.H.; Al-Hadithi, A.I. (2020) Properties of eco-friendly pervious concrete containing polystyrene aggregates reinforced with waste PET fibers. *Innov. Infrastruct. Solut.* 77, 1-16. https://doi.org/10.1007/s41062-020-00323-w.
6. Nazeer, M.; Kapoor, K.; Singh, S.P. (2023) Strength and microstructural properties of pervious concrete made with different powder to aggregate ratios. *Eur. J. Environ. Civ. Eng.* 1–25. https://doi.org/10.1080/19648189.2023.2168763.
7. Ramkrishnan, R.; Abilash, B.; Trivedi, M.; Varsha, P.; Varun, P.; Vishanth, S. (2018) Effect of mineral admixtures on pervious concrete. *Mater. Today Proc.* 5 [11], 24014-24023. https://doi.org/10.1016/j.matpr.2018.10.194.
8. Lu, G.; Liu, P.; Wang, Y.; Fabender, S.; Wang, D.; Oeser, M. (2019) Development of a sustainable pervious pavement material using recycled ceramic aggregate and bio-based polyurethane binder. *J. Clean. Prod.* 220, 1052-1060. https://doi.org/10.1016/j.jclepro.2019.02.184.

9. Yang, J.; Jiang, G. (2003) Experimental study on properties of pervious concrete pavement materials. *Cem. Conc. Res.* 33 [3], 381–386. https://doi.org/10.1016/S0008-8846(02)00966-3.

10. Aman, A.M.N.; Selvarajoo, A.; Chong, S.; Teo, F.Y. (2022) Comparative life cycle assessment of pervious concrete production in Malaysia with natural and recycled aggregate. Innov. *Infrastruct. Solut.* 7, 211. https://doi.org/10.1007/s41062-022-00801-3.

11. Zhang, Y.; Li, H.; Abdelhady, A.; Yang, J. (2020) Effect of different factors on sound absorption property of porous concrete. *Transp. Res. Part D.* 87, 102532. https://doi.org/10.1016/j.trd.2020.102532.

12. Ibrahim, A.; Mahmoud, E.; Yamin, M.; Chowdary, V. (2013) Experimental study on Portland cement pervious concrete mechanical and hydrological properties. *Constr. Build. Mater.* 50, 524-529. https://doi.org/10.1016/j.conbuildmat.2013.09.022.

13. Wang, H.; Li, H.; Liang, X.; Zhou, H.; Xie, N.; Dai, Z. (2019) Investigation on the mechanical properties and environmental impacts of pervious concrete containing fly ash based on the cement-aggregate ratio. *Constr. Build. Mater.* 202, 387-395. https://doi.org/10.1016/j.conbuildmat.2019.01.044.

14. Neptune, A. (2008) Investigation of the effects of aggregate properties and gradation on pervious concrete mixtures. Thesis. 1-154. Retrieved from: https://tigerprints.clemson.edu/cgi/viewcontent.cgi?article=1460&context=all_theses.

15. Kia, A.; Wong, H.S.; Cheeseman, C.R. (2019) High-strength clogging resistant permeable pavement. *Int. J. Pavement Eng.* 22 [3], 271-282. https://doi.org/10.1080/10298436.2019.1600693.

16. Liu, R.; Chi, Y.; Chen, S.; Jiang, Q.; Meng, X.; Wu, K. (2020) Influence of pore structure characteristics on the mechanical and durability behavior of pervious concrete material based on image analysis. *Int. J. Concr. Struct. Mater.* 14, 29. https://doi.org/10.1186/s40069-020-00404-1.

17. El-Hassan, H.; Kianmehr, P.; Zouaoui, S. (2019) Properties of pervious concrete incorporating recycled concrete aggregates and slag. *Constr. Build. Mater.* 212, 164–175. https://doi.org/10.1016/j.conbuildmat.2019.03.325.

18. Wang, K.; Schaefer, V.R.; Kevern, J.T. (2015) Development of mix proportion for functional and durable pervious concrete. *NRMCA Con. Tech. Forum.* 1-12.

19. Mulyono, T.; Anisah, M.T. (2019) Properties of pervious concrete with various types and sizes of aggregate. *MATEC Web Conf.* 276, 01025. https://doi.org/10.1051/matecconf/201927601025.

20. Lim, E.; Hwee, K.; Fang, T. (2013) Effect of mix proportion on strength and permeability of pervious concrete for use in pavement. *J. East. Asia Soc. Tran. Studies.* 1-11.

21. Yeih, W.; Fu, T.C.; Chang, J.J.; Huang, R. (2015) Properties of pervious concrete made with air-cooling electric arc furnace slag as aggregates. *Constr. Build. Mater.* 93, 737–745. https://doi.org/10.1016/j.conbuildmat.2015.05.104.

22. Chopra, M.; Asce, M.; Kakuturu, S.; Asce, A.M.; Ballock, C.; Asce, A.M. (2010) Effect of rejuvenation methods on the infiltration rates of pervious concrete pavements. *J. Hyd. Eng.* 15 [6], 426–33. https://doi.org/10.1061/(ASCE)HE.1943-5584.0000117.

23. Singh, D.; Singh, S.P. (2020) Influence of recycled concrete aggregates and blended cements on the mechanical properties of pervious concrete. *Innov. Infrastruct. Solut.* 5, 66. https://doi.org/10.1007/s41062-020-00314-x.

24. Aliabdo, A.A.; Abd Elmoaty, A.E.M.; Fawzy, A.M. (2018) Experimental investigation on permeability indices and strength of modified pervious concrete with recycled concrete aggregate. *Constr. Build. Mater.* 193, 105–27. https://doi.org/10.1016/j.conbuildmat.2018.10.182.

25. Sun, Z.; Lin, X.; Vollpracht, A. (2018) Pervious concrete made of alkali activated slag and geopolymers. *Constr. Build. Mater.* 189, 797–803. https://doi.org/10.1016/j.conbuildmat.2018.09.067.

26. Aydin, S.; Yazici, H. (2010) Effect of aggregate type on mechanical properties of RPC. *J. Mod. Tech. Eng.* 107 [5], 441-449.

27. Zhang, Z.; Zhang, Y.; Yan, C.; Liu, Y. (2017) Influence of crushing index on properties of recycled aggregates pervious concrete. *Constr. Build. Mater.* 135, 112–118. https://doi.org/10.1016/j.conbuildmat.2016.12.203.

28. Sun, Z.; Lin, X.; Vollpracht, A. (2018) Pervious concrete made of alkali activated slag and geopolymers. *Constr. Build. Mater.* 189, 797–803. https://doi.org/10.1016/j.conbuildmat.2018.09.067.

29. Kayhanian, M.; Anderson, D.; Harvey, J.T.; Jones, D.; Muhunthan, B. (2012) Permeability measurement and scan imaging to assess clogging of pervious concrete pavements in parking lots. *J. Environ. Manage.* 95 [1], 114–23. https://doi.org/10.1016/j.jenvman.2011.09.021.

30. Deo, O.; Asce, M.; Sumanasooriya, M.; Asce, M.; Neithalath, N. (2010) Permeability reduction in pervious concretes due to clogging : experiments and modeling. *J. Mat. Civil Eng.* 22 [7], 741–751. https://doi.org/10.1061/(ASCE)MT.1943-5533.0000079.

31. Bean, E.Z.; Hunt, W.F.; Bidelspach, D.A. (2007) Field survey of permeable pavement surface infiltration rates. *J. Irrig. Drain. Eng.* 133 [3], 249–255. https://doi.org/10.1061/(ASCE)0733-9437(2007)133:3(249).

32. Sandoval, G.F.B.; de Moura, A.C.; Jussiani, E.I.; Andrello, A.C.; Toralles B.M. (2020) Proposal of maintenance methodology for pervious concrete (PC) after the phenomenon of clogging. *Constr. Build. Mater.* 248, 118672. https://doi.org/10.1016/j.conbuildmat.2020.118672.

33. Winston, R.J.; Al-Rubaei, A.M.; Blecken, G.T.; Viklander, M.; Hunt, W.F. (2016) Maintenance measures for preservation and recovery of permeable pavement surface infiltration rate - The effects of street sweeping, vacuum cleaning, high pressure washing and milling. *J. Environ. Manage.* 169, 132–44. https://doi.org/10.1016/j.jenvman.2015.12.026.

34. Sandoval, G.F.B.; Galobardes, I.; Toralles, B.M. (2020) Assessing the phenomenon of clogging of pervious concrete (Pc): Experimental test and model proposition. *J. Buil. Eng.* 29, 101203. https://doi.org/10.1016/j.jobe.2020.101203.

35. Haselbach, L.M.; Asce, M. (2010) Potential for clay clogging of pervious concrete under extreme conditions. *J. Hydr. Eng.* 15 [1], 67–69. https://doi.org/10.1061/(ASCE)HE.1943-5584.0000154.

36. Kia, A.; Wong, H.S.; Cheeseman, C.R. (2017) Clogging in permeable concrete: A review. *J. Environ. Manage.* 193, 221–233. https://doi.org/10.1016/j.jenvman.2017.02.018.

37. IS: 8112-1989 (2013) Specification for 43 grade ordinary portland cement. Bur. Indian Stand. 1-17.

38. IS: 4031 (Part 2)-1999 (2004) Methods of physical tests for hydraulic cement, Determination of fineness by specific surface by Blaine air permeability method. Bur. Indian Stand. 1–13.

39. IS: 4031-1988 (1988) Methods of physical tests for Hydraulic cement. Bu.r Indian Stand. 1-6.

40. IS: 383-1970 (1970) Specification for coarse and fine aggreagtes from natural sources for concrete. Bur. Indian Stand. 1-24.

41. IS: 2386- Part I (2002) Method of test for aggregate for concrete. Particle size and shape. Bur. Indian Stand. 1-26.

42. NRMCA. Guide to Specifying Pervious Concrete.

43. ASTM C1754/C1754-12. (2012) Standard test method for density and void content of hardened pervious concrete. ASTM Stand. 1-3.

44. IS: 516 (1959) Method of tests for strength of concrete. Bur. Indian Stand. 1–30.

45. Haselbach, L.M.; Valavala, S.; Montes, F. (2006) Permeability predictions for sand-clogged Portland cement pervious concrete pavement systems. *J. Environ. Manage.* 81 [1], 42–49.

46. Ramadhansyah, P.J.; Y M.I.M.; Hainin, M.R.; Warid, M.N.M.; Ibrahim, W. (2014) Porous concrete pavement containing nano-silica: Pre-review. 911, 454–458.

47. Yao, A.; Ding, H.; Zhang, X.; Hu, Z.; Hao, R.; Yang, T. (2018) Optimum design and performance of porous concrete for heavy-load traffic pavement in cold and heavy rainfall region of NE China. *Adv. Mater. Sci. Eng.* 2018, 7082897. https://doi.org/10.1155/2018/7082897.

48. Ni, T.Y.; Jiang, C.H.; Tai, H.X., Zhao, G.Q. (2014) Experimental study on sound absorption property of porous concrete pavement layer. *Appl. Mech. Mater.* 507, 238–241. https://doi.org/10.4028/www.scientific.net/AMM.507.238.

49. Neithalath, N.; Marolf, A.; Weiss, J.; Olek, J. (2005) Modeling the influence of pore structure on the acoustic absorption of enhanced porosity concrete. *J. Adv. Concr. Technol.* 3 [1], 29–40.
50. Neithalath, N.; Weiss, J.; Olek, J. (2015) Improving the acoustic absorption of enhanced porosity concrete with fiber reinforcement. *Int. RILEM. Symp. Concr. Sci. Eng.* 1-16.
51. Committee ACI. (2015) ACI 522R-10 Report on pervious concrete. 10, 1-44.
52. Ćosić, K.; Korat, L.; Ducman, V.; Netinger, I. (2015) Influence of aggregate type and size on properties of pervious concrete. *Constr. Build. Mater.* 78, 69–76. https://doi.org/10.1016/j.conbuildmat.2014.12.073.
53. IS : 2386-Part IV. (2016) Methods of test for aggregates for concrete: Mechanical properties. *Bur. Indian Stand. New Delhi.* 1–37.
54. ASTM C131M-20. (2014) C131/C131M-14 Standard test method for resistance to degradation of small-size coarse aggregate by abrasion and impact in the Los Angeles Machine. 5–8.
55. ASTM C 128-01 (2001) Standard test method for density, relative density (Specific gravity), and absorption. 1–6.
56. Bureau of Indian Standards (BIS) (2002) IS:2386-Part V-1963: Methods of test for aggregates for concrete. Indian Stand. 1–14.
57. ASTM C 127–01 (2001) Standard test method for relative density (Specific gravity) and absorption of coarse. 88, 1-6.
58. ASTM C29/C29M − 17a. (2017) Standard test method for bulk density (Unit weight) and Voids in aggregate. 1, 5–9.